

Electronic structure at the C₆₀/metal interface: An angle-resolved photoemission and first-principles study

A. Tamai,^{1,*} A. P. Seitsonen,² F. Baumberger,^{3,*} M. Hengsberger,¹ Z.-X. Shen,³ T. Greber,¹ and J. Osterwalder¹

¹*Physik Institut der Universität Zürich, Winterthurerstrasse 190, 8057 Zürich, Switzerland*

²*IMPMC, CNRS and Université Pierre et Marie Curie, 4 place Jussieu case 115, 75252 Paris, France*

³*Department of Applied Physics, Stanford University, Stanford, California 94305, USA*

(Received 6 September 2007; revised manuscript received 5 November 2007; published 29 February 2008)

High-resolution angle-resolved photoemission reveals a complex electronic structure at the interface between a highly ordered C₆₀ monolayer and the Cu(111) surface. The Shockley-type surface state of the clean substrate is pushed to higher energies by the overlayer and strongly couples to intramolecular C₆₀ phonons. A second interface state with a bandwidth spanning the entire HOMO-LUMO gap disperses with the periodicity of the C₆₀ superstructure. Density functional theory calculations indicate that this state is due to strong hybridization of molecular orbitals and substrate electronic states at the C₆₀/metal interface. This finding sheds light on the issue of self-doping in molecular layers on metal surfaces.

DOI: [10.1103/PhysRevB.77.075134](https://doi.org/10.1103/PhysRevB.77.075134)

PACS number(s): 71.20.Tx, 61.05.js, 79.60.Dp

I. INTRODUCTION

The characterization of C₆₀ molecular layers on metal surfaces has stimulated progress in understanding the complex behavior of correlated fullerene compounds. In solid C₆₀, a variety of different transport properties manifests itself upon intercalation of alkali-metal atoms, ranging from metallic to Mott-Hubbard insulating and superconducting behaviors. Extensive theoretical effort has been dedicated to model the different phases and identify the critical parameters for the transitions.^{1,2} However, basic experimental information on the electronic structure of bulk C₆₀ that could help test existing theories is rare. This is due to the difficulty detecting band dispersion in the presence of orientational disorder, temperature dependent structural transitions, strong electron-phonon coupling, and very small Brillouin zones.

Deposition of C₆₀ molecules on metal surfaces is a way to overcome some of these problems. Because of a balance between molecule-molecule and molecule-substrate interactions, it is possible to grow ordered C₆₀ layers, where the molecules assume well-defined relative orientations. This allowed one to measure the lowest unoccupied molecular orbital (LUMO) dispersion in a K₃C₆₀ monolayer on Ag(111) (Ref. 3) and to investigate the effects of the molecular orientation on the electronic structure.^{4,5} The recent observation that a Jahn-Teller driven metal-insulator transition occurs between a K₃C₆₀ and a K₄C₆₀ monolayer on Au(111) (Ref. 6) supports the idea that much of the interesting properties of bulk C₆₀ should persist in the monolayer systems.

An important issue is the role of the substrate for the electronic properties of the C₆₀ layer. Due to the high electron affinity of C₆₀ and the metallic nature of the substrate, there is significant charge transfer from the substrate to the molecule.⁷ Values between 0.7 and 2 e/C₆₀ have been reported depending on the metal and the surface orientation. This charge transfer can be regarded as a self-doping of the monolayer system. It has received considerable attention because it might provide a route to induce superconductivity⁸ or metal-insulator transitions without the need of chemical doping. Carrier injection due to charge transfer avoids the

structural disorder inherent to chemical doping and suppresses molecular reorientation transitions commonly observed in alkali-metal-doped C₆₀.^{5,9} The C₆₀-noble-metal interaction has been described as predominantly ionic with little hybridization between the molecule and the substrate. However, several authors have pointed out a nontrivial role of the substrate. Scanning tunneling microscopy (STM) studies have shown a significant influence of the underlying metal on the electronic structure of adsorbed C₆₀.^{10,11} In C₆₀/Ag(100), a characteristic splitting of the C₆₀ LUMO into two dominant states has been assigned to the interaction with the substrate.¹² The distribution of the electron density across the C₆₀/metal interface was calculated within density functional theory (DFT) and indicates that the interaction has a covalent rather than purely ionic character.^{13,14}

In this paper, we present the electronic structure of one monolayer of C₆₀ on Cu(111), investigated by angle-resolved photoemission spectroscopy. An extra photoemission peak dispersing in the highest occupied molecular orbital (HOMO)-LUMO gap is interpreted as the signature of hybridization between copper and carbon electronic states. DFT calculations allow us to locate the electronic state at the C₆₀/metal interface. Upon doping with potassium, electron transfer from the alkali atoms reduces charge transfer from the substrate and the hybridization with the substrate decreases.

II. EXPERIMENT

High-resolution photoemission experiments at low-temperature were performed with a Scienta SES 2002 spectrometer at Stanford University, using He I α radiation (21.22 eV) from a microwave driven monochromatized discharge lamp (Gammadata VUV5000). Three differential pumping stages were used in order to reduce the He partial pressure in the measurement chamber to a level near the sensitivity limit of the UHV ion gauges. Energy and angular resolutions were set to 7.5 meV and $\pm 0.15^\circ$ for all measurements. A mechanically polished Cu(111) single crystal was

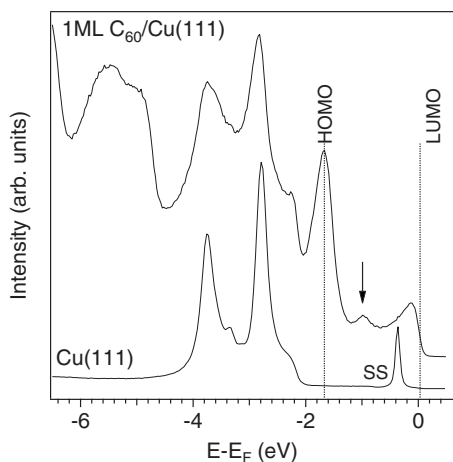


FIG. 1. He $I\alpha$ normal emission spectrum of 1 ML $C_{60}/Cu(111)$ measured at room temperature. The spectrum of the clean $Cu(111)$ substrate is displayed as reference. The arrow indicates the extra peak in the HOMO-LUMO gap, which is described in the text as the interface state. The dotted lines mark the HOMO and LUMO positions.

prepared by standard sputtering and annealing cycles. A good surface quality can be deduced from the width of the Shockley surface state, which was measured in normal emission below 70 meV full width at half maximum (FWHM). C_{60} powder (99.9%) was sublimated from a titanium crucible. The background pressure during evaporation was kept below 5×10^{-10} mbar. Monolayer C_{60} films were prepared by deposition of a multilayer and subsequent annealing of the sample to 600 K. Doping dependent photoemission experiments were performed in a modified VG ESCALAB 220 spectrometer¹⁵ using monochromatized He $I\alpha$ radiation. Potassium was evaporated from a well outgassed SAES getter source onto the C_{60} layer at room temperature.

The $Cu(111)$ surface was chosen because of the small mismatch of only 2% between a multiple of the $Cu-Cu$ nearest-neighbor distance and the intermolecular distance in bulk C_{60} . This might be expected to result in C_{60} films with

properties closely resembling bulk fullerite. The monolayer system exhibits a sharp 4×4 low energy electron diffraction (LEED) pattern. The C_{60} orientation was determined by x-ray photoelectron diffraction.¹⁶ The molecules are adsorbed with a hexagon ring facing the substrate, in two azimuthally equivalent orientations differing by 60° . The presence of two orientations can be rationalized by assuming two different orientational domains on the surface. This adsorption geometry is in agreement with DFT calculations which also indicate the hcp hollow site as the energetically most favorable adsorption site.¹³

III. RESULTS AND DISCUSSION

A. Photoemission data

Figure 1 shows the normal emission photoemission spectra of 1 ML (monolayer) $C_{60}/Cu(111)$ and of the clean substrate measured at room temperature. The spectral weight around 1.7 eV binding energy is due to photoemission from the C_{60} HOMO. Close to the Fermi level (E_F), the high intensity is interpreted as emission from the partially occupied LUMO¹⁷ and the Shockley surface state which is visible around the $\bar{\Gamma}$ point in the first Brillouin zone (Figs. 2 and 3). Around 0.9 eV below E_F , close to the rising tail of the HOMO, there is an additional photoemission peak. It clearly appears after annealing the C_{60} film to 600 K to desorb the multilayer. The same photoemission spectrum was measured by Tsuei *et al.*¹⁸ They noticed that the appearance of the peak at 0.9 eV was associated with the ordering of the 4×4 C_{60} structure, and they interpreted it as originating from the substrate Shockley surface state modified by the presence of the C_{60} overlayer. In the following, we show that this interpretation is unlikely because the extra state disperses outside the sp projected band gap where the surface state is confined. Density functional calculations allow us to identify this extra peak as originating from an interface state caused by strong hybridization between copper states and the carbon atoms facing the substrate.

Constant energy maps measured at 10 K are displayed in Fig. 2. They describe the spectral weight distribution at the

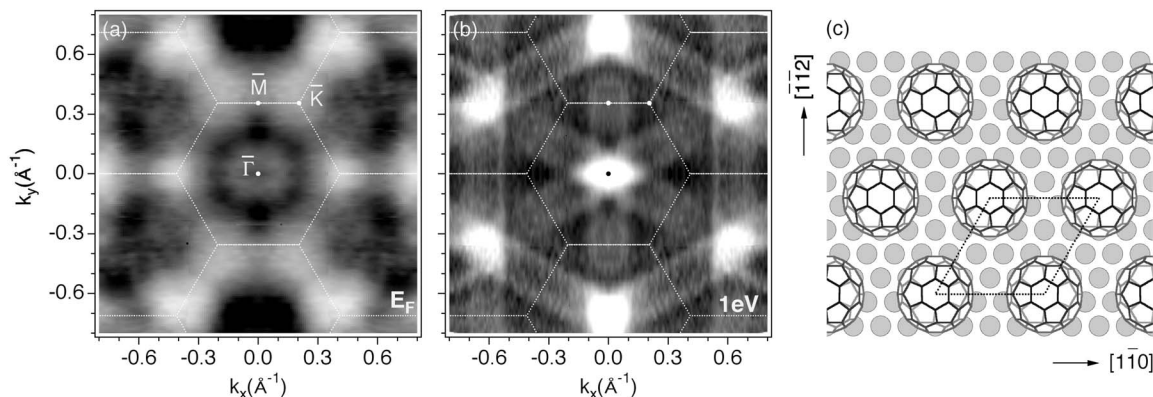


FIG. 2. (a) Fermi surface map of 1 ML $C_{60}/Cu(111)$. (b) Constant energy map at 1 eV binding energy which shows the interface state. Both maps were measured at 10 K. The spectral weight has been integrated in a window of 10 meV width. The straight lines indicate the C_{60} Brillouin zone boundaries. Maximum intensity corresponds to white. (c) Sketch of the direct lattice. C_{60} molecules with the hexagon ring facing the substrate surface form a 4×4 superstructure.

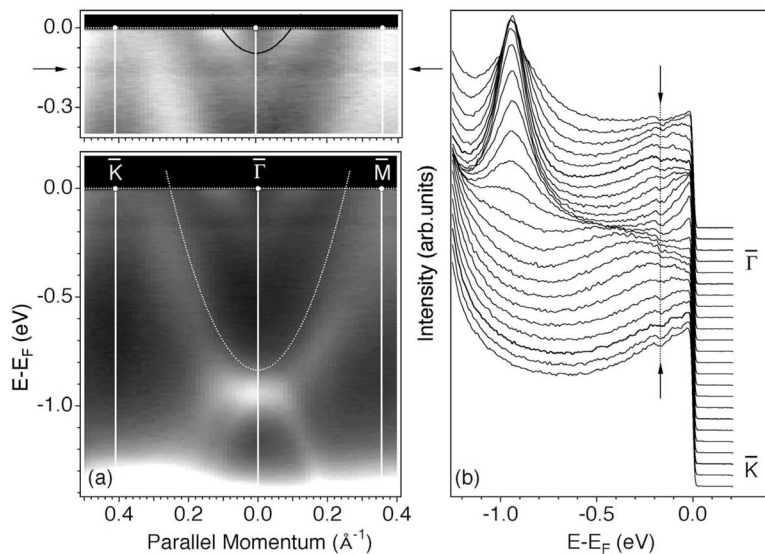


FIG. 3. (a) Dispersion plot of one monolayer of C₆₀ on Cu(111) measured along $\bar{K}\bar{\Gamma}\bar{M}$ (He I α radiation, 10 K). Maximum intensity corresponds to white. The white line indicates the boundaries of the projected *sp*-band gap of Cu(111). In the top panel, the contrast has been enhanced to clearly show the states crossing E_F . The free-electron-like dispersion of the Shockley surface state calculated for the observed value of k_F and the effective mass of the clean substrate is superimposed (black line). (b) Set of equally spaced energy distribution curves along $\bar{\Gamma}\bar{K}$. The arrows in panel (a) and the thin line in panel (b) highlight the dip around 0.16 eV binding energy, which is due to the coupling with the C₆₀ intramolecular phonons.

Fermi level and at 1 eV binding energy, where the intensity of the interface state is high in the normal emission spectrum. The maps have been obtained from $\approx 1 \times 10^4$ high-resolution spectra taken on a uniform k -space grid and integrated over an energy window of 10 meV.

The Fermi surface map [Fig. 2(a)] shows a periodicity in momentum space that matches the C₆₀ Brillouin zones deduced from the 4×4 LEED pattern. The pattern is sixfold symmetric as expected for a two-dimensional C₆₀ layer with sixfold symmetric nearest-neighbor hopping. Around all \bar{K} points of the C₆₀ reciprocal lattice, there is higher photoemission intensity that is related to the electronic structure of the overlayer. However, these features are very broad and diffuse, and it is not possible to identify closed contours separating occupied or unoccupied C₆₀ states. Different intensities at symmetry equivalent points in the surface Brillouin zones are most likely related to different matrix element contributions. In the first C₆₀ Brillouin zone, where the $\bar{\Gamma}$ point coincides with the center of the Cu Brillouin zone, there is an additional bright circle of slightly enhanced intensity around $\bar{\Gamma}$. It is interpreted as the trace of the Shockley surface state, which is visible in the *sp*-band gap at the $\bar{\Gamma}$ point of the clean Cu(111).^{19,20}

The map at 1 eV binding energy shows features related to the extra electronic state within the HOMO-LUMO gap: Well-defined intensity maxima are visible at the centers of the C₆₀ zones and straight stripes connect all $\bar{\Gamma}$ points with the exact sixfold symmetry of the C₆₀ layer [Fig. 2(b)]. We interpret this as the signature of a two-dimensional electronic state with a strongly anisotropic dispersion. The straight line features in the map run along the $[\bar{1}\bar{1}2]$ azimuth and symmetry equivalent directions. They thus represent states that disperse along the C₆₀ nearest-neighbor bond but are localized along the next-nearest-neighbor direction.

Angle-resolved photoemission spectra measured along the $\bar{\Gamma}\bar{K}$ and $\bar{\Gamma}\bar{M}$ directions of the C₆₀ reciprocal lattice are presented in Fig. 3. Between the Fermi level and the tail of the HOMO peak, there are many features which illustrate the complex electronic structure at the C₆₀/metal interface. The

most striking one is the dispersion of the interface peak centered at 0.9 eV in the normal emission spectrum. Around $\bar{\Gamma}$, it is very intense and broad. The momentum linewidth, 0.25 and 0.19 \AA^{-1} along $\bar{\Gamma}\bar{K}$ and $\bar{\Gamma}\bar{M}$, respectively, is indicative of a localized electronic state. For large values of the parallel momentum, the intensity decreases and the peak splits in at least two different branches with opposite group velocities, dispersing down toward the HOMO and up to the Fermi level [Fig. 3(a)]. These states remain outside the projected *sp*-band gap of the Cu(111) electronic structure, the boundaries of which have been highlighted in Fig. 3(a).

At all parallel momenta, the spectra show a pronounced dip at about 0.16 eV which is related to the coupling to the intramolecular phonons of the molecules. Similar structures have been reported for C₆₀/Ag(111) (Refs. 3 and 21) and are characteristic of the C₆₀ photoemission spectra in the metallic phase.²²

Around the $\bar{\Gamma}$ point of the first Brillouin zone, there is a weak dispersing peak that recalls the Shockley-type surface state of Cu(111). Its intensity is almost completely suppressed compared to the clean copper surface, as can be expected by the fact that the escape depth of photoelectron with 16 eV kinetic energy is of the same order of the C₆₀ diameter.^{23,24} The Fermi wave vector k_F is $\approx 0.1 \text{\AA}^{-1}$ and results in an occupation of $\sim 0.01 e^-/\text{surface atom}$, about four times smaller than on the clean Cu(111) substrate.²⁵ The presence of the Shockley surface state after adsorption of an entire C₆₀ monolayer is surprising and has not been reported for other C₆₀/noble metal interfaces. We can exclude to see the surface state of free substrate areas because the C₆₀ layer was prepared by desorbing a multilayer, which is not expected to leave areas of the substrate uncovered. The presence of surface states below ordered adsorbate layers is commonly observed in systems that interact weakly with the substrate such as NaCl/Cu(111) (Ref. 26) or noble gas layers on various metals.²⁷ Adsorbates that hybridize with substrate states such as CO tend to quench surface states.²⁸ Recently, traces of a Shockley-type surface state confined at the molecule/metal interface have been observed in PTCDA-covered Ag (Ref. 29) and Au(111) (Ref. 30) surfaces. Scan-

ning tunneling spectroscopy shows that in these systems, the occupation of the surface state is very sensitive to the degree of order within the molecular layer. We speculate that in $C_{60}/Cu(111)$, the surface state survives in the presence of strong bonding interactions because the hybridized states remain outside the sp projected band gap and no C_{60} -derived states are present around $\bar{\Gamma}$ near E_F as indicated by the low photoemission intensity at the center of the higher C_{60} Brillouin zones [Fig. 2(a)]. Furthermore, our data indicate that there is strong coupling between the surface state and the C_{60} phonons. In the top panel of Fig. 3(a), we have superimposed the typical parabolic dispersion of the surface state calculated for the experimental value of k_F and assuming the same effective mass as on the clean substrate ($m_x=0.41 m_e$). The evident distortion of the experimental dispersion, where a lot of spectral weight is moved outside the one-particle band, and the lineshape changes as a function of parallel momentum [Fig. 3(b)] can be explained by the presence of electron-phonon interactions.³¹ Our data are consistent with significant coupling between the copper surface state and the C_{60} vibrational modes that extend in energy between 20 and 200 meV. A similar coupling was observed between the tungsten (110) surface state and the stretch vibrational mode of adsorbed hydrogen.³²

B. Interface state and density functional theory calculations

The presence of a dispersing band within the HOMO-LUMO gap is unexpected for the band structure of a C_{60} monolayer. In a freestanding layer, these molecular orbitals are expected to form narrow valence and conduction bands, which disperse less than 500 meV and are well separated in energy. This peculiarity could then be a signature of the copper bands or indicate that the C_{60} molecular orbitals have been significantly modified. Final state umklapp, where the photoelectrons are scattered by a reciprocal superlattice vector, could cause copper electronic states to appear with the periodicity of the C_{60} overlayer. However, simulations of this effect considering the dispersion of the copper sp bands at 1 eV binding energy gave a completely different result as compared to the map of Fig. 2(b). A second possibility could be that the HOMO-LUMO gap is smaller because of a stronger molecule-molecule interaction. Band structure calculations of a two-dimensional polymer, where the molecules are covalently bound, indicate that the HOMO- and LUMO-derived states are spread over a larger energy range and the size of the gap is significantly reduced.³³⁻³⁵ However, C_{60} polymerization is expected only when the C_{60} - C_{60} distance is around 9 Å, smaller than the van der Waals radius of the buckyball.³⁶ In the C_{60} monolayer on Cu(111), the nearest-neighbor distance is 10.2 Å and polymerization can safely be excluded. Supported by density functional theory, we propose that the electronic state is the result of the C_{60} /metal interaction which causes strong hybridization between copper and carbon electronic states.

The electronic structure of 1 ML $C_{60}/Cu(111)$ has been calculated using the generalized gradient approximation (DFT-GGA) of Perdew *et al.*³⁷ as the approximation for the exchange-correlation functional.³⁸ We included seven layers

of the substrate and separated the surfaces of the clean slab with about 20 Å of vacuum (supercell geometry). The three uppermost layers of the substrate were allowed to relax. We used a 4×4 mesh of the Monkhorst-Pack k points containing the Γ point.^{41,42} This lead to four independent k points in the irreducible wedge of the Brillouin zone, having the symmetry operations of the C_3 symmetry group. The occupation numbers were broadened with a Fermi-Dirac distribution with the temperature corresponding to 50 meV.

In order to investigate the electronic structure at the interface, we projected the Kohn-Sham orbitals of the surface system on the atomic orbitals of the six lowermost carbon atoms of the molecule facing the copper surface. We calculated the square amplitude

$$I_\mu(\varepsilon, k_\parallel) = \sum_i \delta(\varepsilon - \varepsilon_{i, k_\parallel}) |\langle \phi_\mu | \psi_{i, k_\parallel} \rangle|^2, \quad (1)$$

where μ indicates the orbital (all s and p orbitals ϕ_μ of the six lowermost carbon atoms), i is the band index, $\varepsilon_{i, k_\parallel}$ the eigenvalues from the DFT calculation, and ψ_{i, k_\parallel} the Kohn-Sham states. The result for $k_z=0$ and $k_\parallel=\bar{\Gamma}$ is presented in Fig. 4(a). The normal emission valence band spectrum of $C_{60}/Cu(111)$ measured at room temperature is displayed for comparison in Fig. 4(b). In order to account for the different values of the HOMO-LUMO gap in DFT and photoemission, the two energy scales have been aligned at the Fermi level and rescaled in a way that the peak at 1.2 eV matches the HOMO photoemission peak centered at 1.7 eV binding energy. In the calculation [Fig. 4(a)], the peaks around 1.2 eV and close to the Fermi level represent the contributions of the six lowermost carbon atoms to the HOMO and LUMO charge density. Interestingly, there is also a very pronounced peak at about 0.7 eV, which compares very well with the interface state in the photoemission spectrum.

By multiplying the density of states projected on the lowest carbon atoms with the density of states projected on the topmost Cu layer, we quantified the contribution of the copper substrate to the electronic states described above. This should give us a measure if a state $\epsilon(\mathbf{k})$ has weight both on the carbon and the nearest-neighbor Cu atoms. The result of the calculation for $\mathbf{k}=\bar{\Gamma}$ is shown in the inset of Fig. 4(a). Because of the adsorption geometry of the molecule (hcp hollow site), the interface atoms can be described by two Cu-C pairs of different bond lengths [see black and white dots in the sketch of Fig. 4(a)]. The peak at 0.7 eV mainly derives from the d_{z^2} , s , and p states of the short Cu-C pairs (solid line). The local density of states at 0.5 eV is mostly due to the p and d states of the longer Cu-C pairs.

The wave functions for a selection of states in the HOMO-LUMO gap calculated at $\bar{\Gamma}$ are presented in Fig. 5. At 1.13 eV, the valence electrons are distributed all around the C_{60} molecule as expected for energy values that correspond to the HOMO. Moving to lower binding energies, the charge localizes at the interface involving the bottom part of the molecules and the first few copper layers. We conclude that the extra electronic state is located at the C_{60} /metal interface and is the result of strong hybridization between the

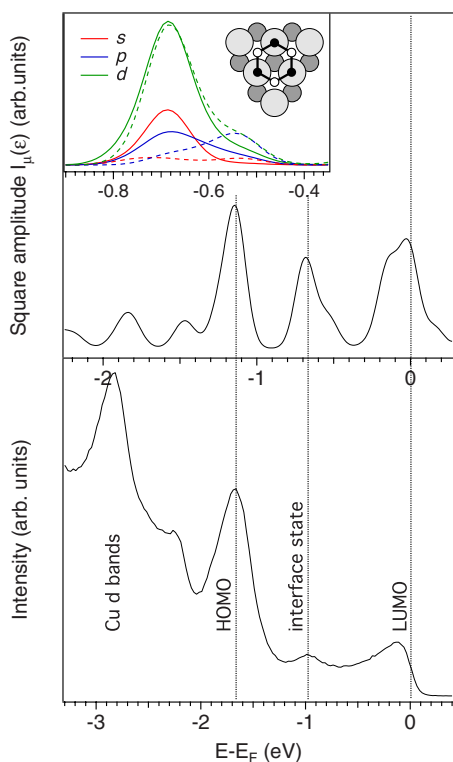


FIG. 4. (Color online) (a) Square amplitude of the Kohn-Sham wave functions projected on the atomic orbitals of the six lowermost carbon atoms facing the substrate surface and calculated at $k_{\parallel}=\bar{\Gamma}$ [sum of s and p contributions in Eq. (1)]. Inset: density of states projected on the topmost Cu layer multiplied by the density of states projected on the carbon atoms at the bottom of a C₆₀ molecule. Solid and dashed lines represent the contributions of Cu-C pairs with short and long bond lengths, 2.099 and 2.517 Å, respectively. A sketch of the adsorption geometry is displayed too. (b) Room-temperature normal emission valence band spectrum of 1 ML C₆₀/Cu(111). The energy scales (a) of the calculation and (b) of the experimental data have been aligned at the Fermi level and rescaled to account for the two different values of the gap.

copper bands and the atomic orbitals of the carbon atoms facing the (111) surface.

An interesting aspect is that the interface state appears very prominent on the Cu(111) surface while data from the other noble metals do not show such pronounced hybridization. Electronic states within the HOMO-LUMO gap have been observed for C₆₀/Au(778) at partial coverage but have been associated with local defects (isolated molecules or cluster edges) and did not show any energy dispersion.⁴⁴ If we compare the properties of 1 ML of C₆₀ on the three (111) surfaces of Cu, Ag, and Au, we see that the C₆₀-C₆₀ distance is 2% larger on Cu than on Ag and Au. Both the adsorption energies and the amount of charge transfer⁴³ indicate that the strength of the bond decreases in moving from Cu to Ag and Au, which is consistent with higher hybridization for a copper substrate. The fact that the electronic structures of the three surfaces are different may play an important role. The Ag d band lies at about 2 eV higher binding energy than the Cu and Au d bands, and this has been considered to cause different degrees of hybridization with the HOMO-1 level of

C₆₀.⁴⁵ However, if the only criterion for the appearance of hybridization were the energy position of the d band, the interface state should be well visible also on Au, while photoemission experiments do not report an extra peak for C₆₀ on Au(111).⁴³ Two other aspects of the structure of the C₆₀ monolayer may contribute to the stronger hybridization on Cu(111): (i) The larger distance between the molecules causes a reduction of the intermolecular hopping. For smaller overlap between the molecular orbitals and therefore weaker C₆₀-C₆₀ interaction, a higher mixing between copper and carbon states can be expected. (ii) The different arrangement of the C₆₀ hexagonal layer with respect to the (111) surface, 4×4 on Cu(111) and $2\sqrt{3} \times 2\sqrt{3}R30^\circ$ on Ag and Au(111), may affect the electronic coupling at the interface. In all three metals, the Fermi surface is threefold symmetric around the [111] direction, but in Ag and Au, it is rotated by 30° with respect to the C₆₀ overlayer. This may result in a less efficient overlap between the metal and C₆₀ states, thus reducing the hybridization at the interface. This is in line with the fact that photoemission experiments performed on polycrystalline copper samples did not show the interface state.⁴⁵

C. Dispersion of the interface state

The observation of strongly anisotropic dispersion of this interface state [Fig. 2(b)] is remarkable and unexpected for a perfect hexagonal layer. The straight bands connecting all $\bar{\Gamma}$ points of the C₆₀ Brillouin zone are indicative of one-dimensional dispersion along the molecule-molecule nearest-neighbor direction, although there is no obvious one-dimensional element in the geometrical arrangement of the molecular layer. Local one-dimensional ordering has been reported for submonolayer growth of C₆₀/Cu(111) due to an adsorbate-induced reconstruction,⁴⁶ while all existing data from complete monolayers indicate the formation of the well-ordered 4×4 structure without additional superstructures. An alternative candidate for introducing linearly coupled molecular chains may be identified from the strong influence that the relative orientation of neighboring molecules has on the band dispersion.⁴⁷ In this system, there is a structural degree of freedom, given by the two inequivalent orientations of the fullerenes in the monolayer,¹⁶ one rotated by 60° from the other. One can then consider a hexagonal lattice of molecules containing chains with common fullerene orientation. Along these chains, coherent coupling of electronic states is possible, leading to the strongly anisotropic dispersion. This may therefore be a unique system for studying the influence of orientational disorder on electronic band formation.

D. Hybridization and charge transfer

The degree of hybridization between the molecules and the copper substrate is very sensitive to the occupation of the C₆₀ LUMO, which can be varied upon K doping.

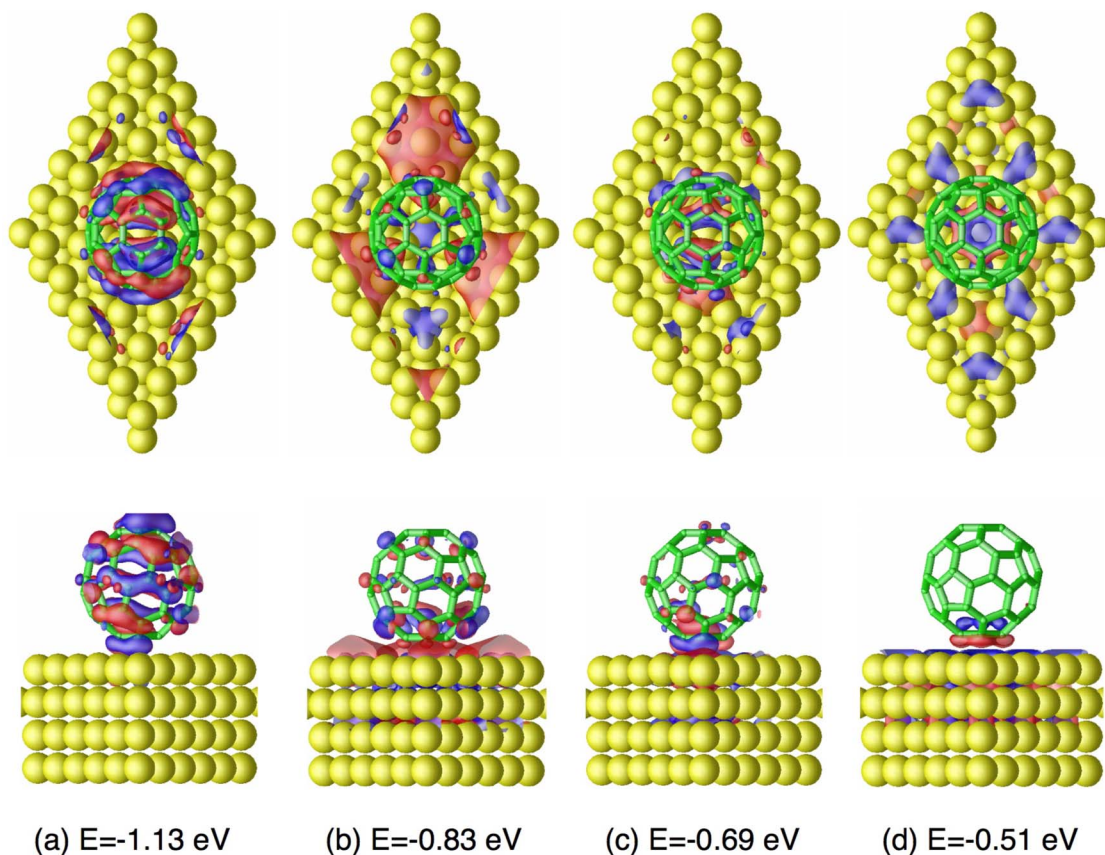


FIG. 5. (Color online) The Kohn-Sham orbitals of the valence electron states at the Γ point calculated at different energies below the Fermi energy (1.13, 0.83, 0.69, and 0.51 eV from left to right). The red and blue isosurfaces denote different signs of the wave function. Only the topmost four layers of the substrate are shown.

A series of normal emission spectra has been recorded during potassium deposition onto the sample at room temperature. Figure 6(a) displays a two-dimensional plot of the

valence band spectrum of $C_{60}/Cu(111)$ as a function of the binding energy and the K evaporation time. For very low amounts of potassium on the surface, the intensity at the

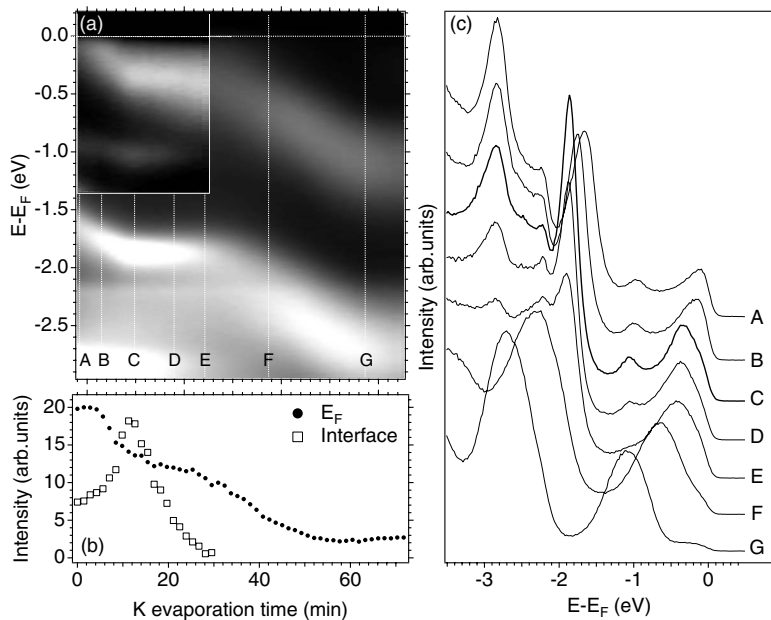


FIG. 6. (a) Grayscale two-dimensional plot of the room-temperature normal emission valence band spectrum displayed as a function of binding energy and potassium evaporation time. For low K doping and small binding energy, the contrast has been enhanced by a factor of 3; high intensity corresponds to white. (b) Intensity at the Fermi level (black dots) and of the interface state (squares) as a function of the potassium evaporation time (c) Comparison of normal emission spectra for different doping levels of the C_{60} LUMO.

Fermi level first slightly increases and then decreases [Fig. 6(b)]; the maximum of the LUMO peak shifts to higher binding energy until it reaches a plateau at about 0.35 eV below E_F . The same energy shift is visible for the C₆₀ HOMO, which is consistent with a rigid band shift upon electron doping into the C₆₀ conduction band. The interface state, however, moves only 100 meV toward higher binding energies and its intensity increases by more than a factor of 2 before the state loses weight again and disappears below the broad LUMO peak. The latter indicates that potassium deposition hampers hybridization between the substrate and the C₆₀ molecule especially at high doping. This is in line with the results of Hoogenboom *et al.* for K-doped C₆₀ monolayers on polycrystalline noble metals surfaces.⁴⁵ In that case, hybridization was inferred by the broadening of the HOMO-1 peak and was found to disappear at high doping when the overlayer completely suppresses the substrate signal. We also observed that K evaporation onto the sample kept at 470 K results in a rapid quenching of the interface state. The higher mobility of the dopant ions at this temperature may result in a more efficient diffusion of potassium underneath the C₆₀ layer and cause a reduction of C₆₀-Cu hybridization.

The present data shed light on the issue of charge transfer at the C₆₀/noble metal interface. So far, in all photoemission studies of C₆₀ monolayers on metal surfaces, the intensity close to the Fermi level has been interpreted as emission from the partially occupied C₆₀ LUMO and the contribution of the substrate was neglected. Based on these assumptions, different methods have been developed to calibrate the occupancy of the C₆₀ LUMO due to charge transfer.^{48,49} However, the evidence of electronic hybridization at the interface and the fact that the Shockley surface state is visible in the first C₆₀ Brillouin zone suggest that this approach may overestimate the charge transfer. DFT calculations of the charge transfer from the metal to the molecules generally yield smaller values than the ones obtained experimentally based on photoemission spectra. In the case of C₆₀/Cu(111), this difference is remarkable. The charge state of the molecule calculated in DFT is $-0.8 e$.¹³ The experimental value reported by Tsuei *et al.* upon evaluating the integrated intensity close to E_F is $-1.5-2 e/C_{60}$. Our calibration based on the data of Fig. 6(a) following the procedure defined by Cepek *et al.*⁴⁸ indicates that the charge transfer is about $-2.9 e/C_{60}$. The significant disagreement between experiments and theory can be explained by the fact that in the presence of strong hybridization, the occupied states close to the Fermi level do not actually contribute a *full* electron to the molecule because the same states have also significant weight on the Cu atoms.

The above results demonstrate that an absolute determination of the C₆₀ charge state in strongly hybridized monolayer systems is not straightforward. However, by looking at the photoemission spectral line shape, it is possible to estimate the metallicity or an insulating character of the monolayer at different doping levels. In a single-particle picture,

the system should be metallic for any partial filling of the LUMO. Electron-electron correlations and electron-lattice interactions drastically modify the phase diagram, and a clear metallic phase is expected only at half filling of the conduction band.¹ Representative normal emission spectra for different doping levels of the C₆₀ LUMO are displayed in Fig. 6(c). Upon doping with potassium, most of the spectral weight moves from the Fermi level toward higher binding energy, suggesting that the most metallic phase occurs at very low K doping. This is also in agreement with the changes in width of the HOMO-derived peak. From spectrum A to C, the FWHM decreases from 350 to 200 meV; upon further doping, the HOMO broadens up to 500 meV for a fully doped C₆₀ monolayer (spectrum G). In the insulating C₆₀ phases, the broad line shape of the spectral features is due to multiphonon excitations. The photohole is not efficiently screened and heavily couples to the vibrational modes of the cage.⁵⁰ At high doping, the coupling to the optic vibrations of the K ions broadens the spectrum too.²² A narrow HOMO-derived peak can occur when the photohole is efficiently screened by, e.g., the electrons in the conduction band. Screening should be maximum in the most metallic phase.

IV. CONCLUSIONS

We have presented angle-resolved photoemission data from 1 ML of C₆₀ on Cu(111). In this system, the interaction at the molecule/metal interface significantly modifies the band structure. The Shockley surface state is pushed to higher energies and strongly couples to the intramolecular C₆₀ phonons. An additional photoemission peak appears within the HOMO-LUMO gap and disperses down toward the HOMO and up to the Fermi level. DFT calculations indicate that the interface state is due to strong electronic hybridization between the six carbon atoms facing the surface and the first few layers of copper atoms. Because of this hybridization, the spectral weight at the Fermi level is not unambiguously related to the C₆₀ electronic structure since the same states have significant weight on the copper atoms and the two electronic structures cannot be decoupled. The present study has important implications for the correct interpretation of the Fermi surface of molecular layers on metals and shows that although adsorption on metal surface has the advantage to produce highly ordered molecular systems, there are cases where the electronic properties of the adsorbed molecule change significantly. Very recently, mixing of electronic states at the interface has been reported also in pentacene monolayers adsorbed on copper.^{51,52}

ACKNOWLEDGMENTS

We would like to thank W. Meewasana for technical assistance during the experiment at Stanford University. This work was supported by the Swiss National Science Foundation.

- *Present address: School of Physics and Astronomy, University of St. Andrews, North Haugh, St. Andrews, KY16 9SS, United Kingdom
- †anna.tamai@st-andrews.ac.uk
- ¹O. Gunnarsson, *Alkali-Doped Fullerenes: Narrow-Band Solids With Unusual Properties* (World Scientific, Singapore, 2004).
 - ²N. Manini and E. Tosatti, arXiv:cond-mat/0602134 (unpublished).
 - ³W. L. Yang *et al.*, *Science* **300**, 303 (2003).
 - ⁴V. Brouet, W. L. Yang, X. J. Zhou, H. J. Choi, S. G. Louie, M. L. Cohen, A. Goldoni, F. Parmigiani, Z. Hussain, and Z.-X. Shen, *Phys. Rev. Lett.* **93**, 197601 (2004).
 - ⁵A. Tamai, A. P. Seitsonen, R. Fasel, Z.-X. Shen, J. Osterwalder, and T. Greber, *Phys. Rev. B* **72**, 085421 (2005).
 - ⁶A. Wachowiak, R. Yamachika, K. H. Khoo, Y. Wang, M. Grobis, D.-H. Lee, Steven G. Louie, and M. F. Crommie, *Science* **310**, 468 (2005).
 - ⁷S. Modesti, S. Cerasari, and P. Rudolf, *Phys. Rev. Lett.* **71**, 2469 (1993).
 - ⁸C. Cepek, I. Vobornik, A. Goldoni, E. Magnano, G. Selvaggi, J. Kroeger, G. Panaccione, G. Rossi, and M. Sancrotti, *Phys. Rev. Lett.* **86**, 3100 (2001).
 - ⁹Y. Wang, R. Yamachika, A. Wachowiak, M. Grobis, K. H. Khoo, D.-H. Lee, S. G. Louie, and M. F. Crommie, *Phys. Rev. Lett.* **99**, 086402 (2007).
 - ¹⁰C. Silien, N. A. Pradhan, W. Ho, and P. A. Thiry, *Phys. Rev. B* **69**, 115434 (2004).
 - ¹¹X. Lu, M. Grobis, K. H. Khoo, Steven G. Louie, and M. F. Crommie, *Phys. Rev. B* **70**, 115418 (2004).
 - ¹²X. Lu, M. Grobis, K. H. Khoo, Steven G. Louie, and M. F. Crommie, *Phys. Rev. Lett.* **90**, 096802 (2003).
 - ¹³Lin-Lin Wang and Hai-Ping Cheng, *Phys. Rev. B* **69**, 045404 (2004).
 - ¹⁴Lin-Lin Wang and Hai-Ping Cheng, *Phys. Rev. B* **69**, 165417 (2004).
 - ¹⁵T. Greber, O. Raetz, T. J. Kreutz, P. Schwaller, W. Deichman, E. Wetli, and J. Osterwalder, *Rev. Sci. Instrum.* **68**, 4549 (1997).
 - ¹⁶R. Fasel, P. Aebi, R. G. Agostino, D. Naumovic, J. Osterwalder, A. Santaniello, and L. Schlapbach, *Phys. Rev. Lett.* **76**, 4733 (1996).
 - ¹⁷S. J. Chase, W. S. Bacsa, M. G. Mitch, L. J. Pilione, and J. S. Lannin, *Phys. Rev. B* **46**, 7873 (1992).
 - ¹⁸K.-D. Tsuei, J.-Y. Yuh, C.-T. Tzeng, R.-Y. Chu, S.-C. Chung, and K.-L. Tsang, *Phys. Rev. B* **56**, 15412 (1997).
 - ¹⁹P. O. Gartland and B. J. Slagsvold, *Phys. Rev. B* **12**, 4047 (1975).
 - ²⁰S. D. Kevan and R. H. Gaylord, *Phys. Rev. B* **36**, 5809 (1987).
 - ²¹A. Goldoni, C. Cepek, E. Magnano, A. D. Laine, S. Vandr e, and M. Sancrotti, *Phys. Rev. B* **58**, 2228 (1998).
 - ²²S. Wehrli, T. M. Rice, and M. Sigrist, *Phys. Rev. B* **70**, 233412 (2004).
 - ²³M. P. Seah and W. A. Dench, *Surf. Interface Anal.* **1**, 21 (1979).
 - ²⁴In the normal emission spectra of Figs. 1 and 3, the different intensity of electronic states close to E_F relative to the interface state is due to the fact that the angle of incidence of the light to the sample in the Scienta and the VG ESCALAB systems is different.
 - ²⁵F. Baumberger, T. Greber, and J. Osterwalder, *Phys. Rev. B* **64**, 195411 (2001).
 - ²⁶J. Repp, G. Meyer, and K. H. Rieder, *Phys. Rev. Lett.* **92**, 036803 (2004).
 - ²⁷J.-Y. Park, U. D. Ham, S. J. Kahng, Y. Kuk, K. Miyake, K. Hata, and H. Shigekawa, *Phys. Rev. B* **62**, R16341 (2000).
 - ²⁸F. Baumberger, T. Greber, B. Delley, and J. Osterwalder, *Phys. Rev. Lett.* **88**, 237601 (2002).
 - ²⁹R. Temirov, S. Soubatach, A. Luican, and F. S. Tautz, *Nature (London)* **444**, 350 (2007).
 - ³⁰J. Kr oger, H. Jensen, R. Berndt, R. Rurali, and N. Lorente, *Chem. Phys. Lett.* **438**, 249 (2007).
 - ³¹I. Barke, F. Zheng, A. R. Konicek, R. C. Hatch, and F. J. Himpsel, *Phys. Rev. Lett.* **96**, 216801 (2006).
 - ³²E. Rotenberg, J. Schaefer, and S. D. Kevan, *Phys. Rev. Lett.* **84**, 2925 (2000).
 - ³³K. Harigaya, *Chem. Phys. Lett.* **242**, 585 (1995).
 - ³⁴Susumu Okada and Atsushi Oshiyama, *Phys. Rev. B* **68**, 235402 (2003).
 - ³⁵T. Miyake and S. Saito, *Chem. Phys. Lett.* **380**, 589 (2003).
 - ³⁶J. Nakamura, T. Nakayama, S. Watanabe, and M. Aono, *Phys. Rev. Lett.* **87**, 048301 (2001).
 - ³⁷J. P. Perdew, J. A. Chevary, S. H. Vosko, K. A. Jackson, M. R. Pederson, D. J. Singh, and C. Fiolhais, *Phys. Rev. B* **46**, 6671 (1992).
 - ³⁸In particular, we used the code VASP [Vienna *ab initio* simulation package; G. Kresse and J. Furthm ller, *Comput. Mater. Sci.* **6**, 15 (1996)]. The wave functions were expanded in plane waves up to the cutoff energy of 37 Ry, and the interaction between the valence and core electrons was taken into account via the projected augmented method (Refs. 39 and 40).
 - ³⁹P. E. Bl ochl, *Phys. Rev. B* **50**, 17953 (1994).
 - ⁴⁰G. Kresse and D. Joubert, *Phys. Rev. B* **59**, 1758 (1999).
 - ⁴¹H. J. Monkhorst and J. D. Pack, *Phys. Rev. B* **13**, 5188 (1976).
 - ⁴²S. L. Cunningham, *Phys. Rev. B* **10**, 4988 (1974).
 - ⁴³C.-T. Tzeng, W.-S. Lo, J.-Y. Yuh, R.-Y. Chu, and K.-D. Tsuei, *Phys. Rev. B* **61**, 2263 (2000).
 - ⁴⁴F. Schiller, M. Ruiz-Os es, J. E. Ortega, P. Segovia, J. Mart nez-Blanco, B. P. Doyle, V. P erez-Dieste, J. Lobo, N. N eel, R. Berndt, and J. Kr oger, *J. Chem. Phys.* **125**, 144719 (2006).
 - ⁴⁵B. W. Hoogenboom, R. Hesper, L. H. Tjeng, and G. A. Sawatzky, *Phys. Rev. B* **57**, 11939 (1998).
 - ⁴⁶W. W. Pai, C.-L. Hsu, M. C. Lin, K. C. Lin, and T. B. Tang, *Phys. Rev. B* **69**, 125405 (2004).
 - ⁴⁷A. Tamai, A. P. Seitsonen, T. Greber, and J. Osterwalder, *Phys. Rev. B* **74**, 085407 (2006).
 - ⁴⁸C. Cepek, M. Sancrotti, T. Greber, and J. Osterwalder, *Surf. Sci.* **454**, 467 (2000).
 - ⁴⁹L. H. Tjeng, R. Hesper, A. C. L. Heessels, A. Heeres, H. T. Jonkman, and G. A. Sawatzky, *Solid State Commun.* **103**, 31 (1997).
 - ⁵⁰P. A. Br uhwiler, A. J. Maxwell, P. Baltzer, S. Andersson, D. Arvanitis, L. Karlsson, and N. Martensson, *Chem. Phys. Lett.* **279**, 85 (1997).
 - ⁵¹A. Ferretti, C. Baldacchini, A. Calzolari, R. Di Felice, A. Ruini, E. Molinari, and M. G. Betti, *Phys. Rev. Lett.* **99**, 046802 (2007).
 - ⁵²H. Yamane, D. Yoshimura, E. Kawabe, R. Sumii, K. Kanai, Y. Ouchi, N. Ueno, and K. Seki, *Phys. Rev. B* **76**, 165436 (2007).